

Chemical Remanent Magnetism Related to the Dead Sea Rift: Evidence From Precambrian Igneous Rocks of Mount Timna, Southern Israel

SHMUEL MARCO,^{1,2} HAGAI RON,² ALAN MATTHEWS,¹ MICHAEL BEYTH,³ AND ODED NAVON¹

A paleomagnetic and mineralogical study of shallow intrusive basement rocks on Mount Timna (Arabo Nubian Massif in Sinai) shows that although all the igneous rocks are of late Precambrian age, a remanent magnetic direction similar to the subrecent field (Miocene to present) is identified in samples of quartz-monzodiorite, monzodiorite, dikes of various composition, and altered gabbro. The average direction of these rock units is (*D/I*) 359°/41°, $\alpha_{95}=4^\circ$, and the pole is at 83.6°N, 223.2°E. The "subrecent" direction appears both as an overprint direction and as the sole stable vector in dolerite, rhyolite, and andesite dikes. The magnetic mineral assemblage of these rocks includes secondary minerals, such as hematite and goethite, which formed by oxidation and hydration of the original magnetite and Ti-magnetite. The subrecent direction is interpreted to have been acquired as a chemical remanent magnetization (CRM) by hydrothermal activity and circulation of thermal brines through fractures related to the adjacent Dead Sea transform. The hydrothermal activity occurred before uplift and erosion exposed the basement rocks, i.e., in the middle Miocene, during the early stages of activity of the Dead Sea rift. The north trending declinations indicate that Mount Timna has not rotated about a vertical axis after acquisition of the CRM, a conclusion that confirms a previous structural analysis. An absence of reversals implies that the duration of CRM acquisition was probably less than ~1 m.y., the maximum length of normal polarities since the Oligocene. Other field directions were found in an alkali granite (one site, 343°/14°, $\alpha_{95}=22^\circ$), in a dolerite dike (one site, 318°/0°, $\alpha_{95}=2^\circ$) and in a gabbro (seven sites, 303°/56°, $\alpha_{95}=6^\circ$). The field direction in the granite is similar to that for Early Cretaceous, a time of magmatic activity in Timna. Northwest trending declinations and shallow inclinations found in several samples of the dikes are carried by unaltered parts of the rocks. These directions are interpreted as late Precambrian-Early Cambrian in age, indicating a near-equatorial location of the region at that time.

INTRODUCTION

The characteristic remanent magnetization of a rock unit is primarily a result of its thermal history and the formation processes of its constituent magnetic minerals. The use of paleomagnetic data for constraining tectonic models is valid, provided the age of the magnetization is well defined. Magnetic components should be correlated with dated processes of formation or any subsequent modification of the magnetic minerals, before the paleomagnetic data can be correctly interpreted.

The present study provides an example of the problems of paleomagnetic interpretation from the Precambrian Arabo Nubian Massif of Arabia and NE Africa and may explain part of the uncertainty noted in the Precambrian apparent polar wander path (APWP) of Africa. A number of articles conclude that the Precambrian Arabo Nubian Massif [Kennedy, 1964] (Figure 1) formed by accretion of mature island arcs between ~950 and 650 Ma and subsequently was cratonized during the "batholithic stage" of the Pan-African orogeny at around 650–550 Ma. This stage included widespread plutonic activity throughout the Massif and to a lesser extent in northern Africa. The Arabo Nubian Massif has been attached to Africa since the beginning

of the batholithic stage [Benton, 1985; Vail, 1983]. The paleomagnetic poles of late Precambrian rocks from the Massif should therefore coincide with those from Africa. Several authors determined the late Precambrian position of Africa by combining biogeographic, climatically sensitive lithofacies, and paleomagnetic data: Burrett *et al.* [1990] and Scotese and Barrett, [1990] showed that the Arabian Peninsula in the late Precambrian was at ~30°S latitude and rotated 90° counterclockwise relative to its present position. Piper [1987] used selected paleomagnetic poles from the Precambrian shields of Gondwanaland to illustrate an APWP for the interval 700 Ma to Lower Cambrian: poles from 650 to 580 Ma plot as a southeast trending swath from the equator toward ~30°S, where the path turns north, crossing the equator in Early Cambrian time. The paleomagnetic data from Africa are poorly constrained [Piper, 1989], and a set of reliability criteria that assigns a quality factor between 0 and 7 assigns only 2 to about 80% of the late Precambrian African data [Van der Voo, 1990]. The paleomagnetic data from Precambrian rocks of Africa cannot be considered to provide a well-constrained APWP.

The present work integrates paleomagnetic with mineralogical studies of the upper Precambrian intrusive Mount Timna basement complex in Sinai (Figure 1). Together with other basement outcrops in southern Israel and Jordan, they form the northern extremity of the Arabo Nubian Massif exposures surrounding the Red Sea. The Timna igneous complex is located at the margin of the Dead Sea transform in a region of well-documented hydrothermal activity and copper, uranium, and manganese mineralization. The mineralization is in part related to the transform, but also occurs throughout the region's geological history [Bar-Matthews, 1986; Beyth, 1987b; Segev, 1985]. The arid climate in southern Israel with about 25 mm of annual precipitation bears on the nature of weathering and erosion.

¹ Institute of Earth Sciences, The Hebrew University, Jerusalem, Israel.

² Institute for Petroleum Research and Geophysics, Holon, Israel.

³ Geological Survey of Israel, Jerusalem.

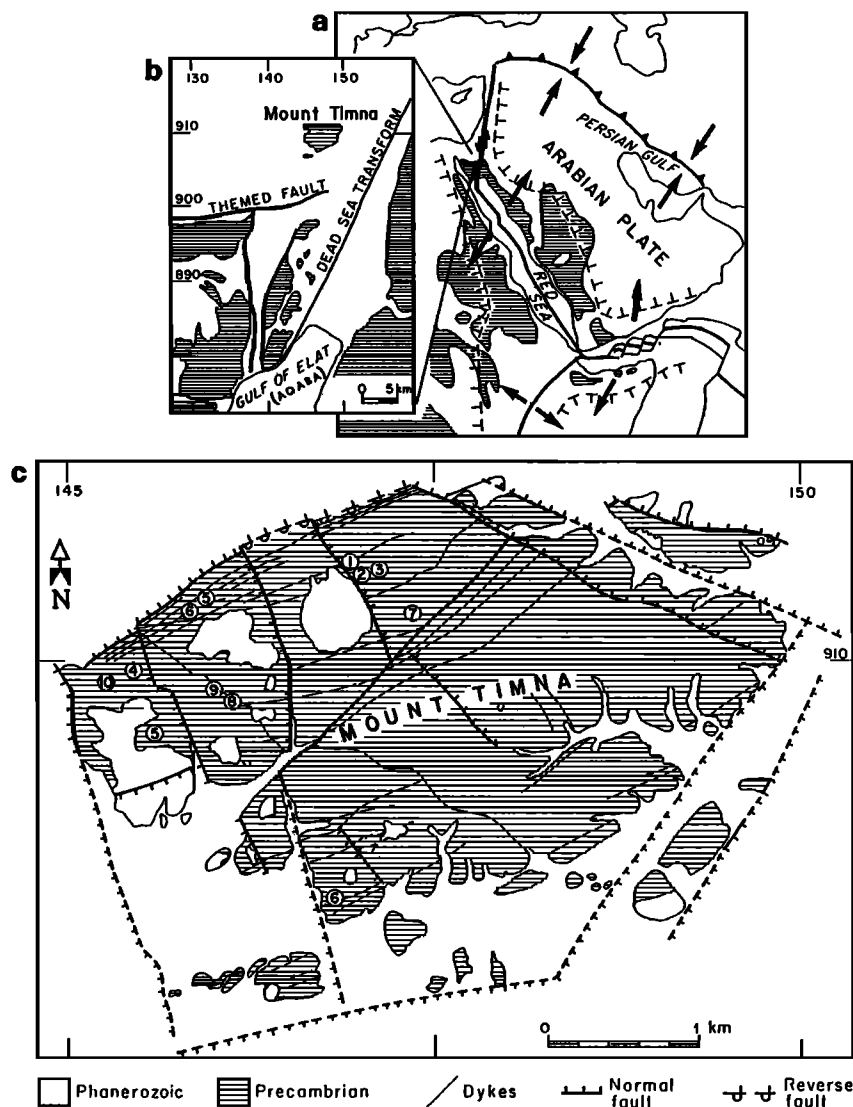


Fig. 1.(a) Map showing outcrops of the Arabo Nubian Massif, (b) the Massif outcrops in southern Israel [after Garfunkel, 1980], (c) generalized geological map of Mount Timna [after Beyth, 1990]. Sampling locations are marked with numbered circles which refer to Tables 1 and 2.

In view of their postemplacement history, our study explores the extent to which the igneous rocks of Timna still retain an original Precambrian magnetization. We show that the upper Precambrian igneous rocks acquired chemical remanent magnetizations (CRM) during a short period ($<10^6$ years) of subrecent hydrothermal activity. Similar conditions might have affected other Precambrian rock units in Africa as well.

GEOLOGICAL HISTORY OF THE TIMNA COMPLEX

Mount Timna is a 20 km² pentagonal uplifted basement block located on the western margin of the southern part of the Dead Sea rift, some 30 km north of the Gulf of Elat (Aqaba) at 29.8°N, 34.9°E (Figure 1). The mountain is the core of a domal structure and is mainly composed of Upper Precambrian shallow intrusive rocks ranging in composition from gabbro (olivine-norite) to calcalkaline and alkali-granites. Swarms of dikes of various composition and orientation are common. Several fracture systems are also common and usually closely

spaced at intervals of centimeters to decimeters. Most of the rocks have a fresh appearance. Precambrian metamorphic and volcanic rocks are absent in Timna [Beyth, 1987a].

A Rb-Sr isochron age of 592 ± 7 Ma was reported [Halpern and Tristan, 1981] for an unspecified "Timna granite," whereas single zircon $^{207}\text{Pb}/^{206}\text{Pb}$ ages [Kröner and Beyth, 1990] give slightly older ages: 625 ± 5 Ma for the calcalkaline granite, 611 ± 10 and 610 ± 8 Ma for the gabbro and diorite respectively and 609 ± 10 Ma for the alkali granite. Field relations show that the quartz monzodiorite is the youngest pluton [Shpitser et al., 1991] and it is intruded only by dolerite dikes that are the latest Precambrian intrusions [Baer and Beyth, 1990]. Radiometric ages and stratigraphic position show that the igneous complex was shaped during the post-orogenic batholithic phase of the Arabo-Nubian crust formation [Bentor, 1985]. At the beginning of this phase, the Arabo Nubian Massif became part of the older African Massifs. It remained part of Africa until the Tertiary, when the Syrian-African rifting and continental breakup processes commenced.

The transition from orogenic to cratonic conditions occurred in the Early Cambrian when uplift and erosion of 2-4 km exposed the plutonic rocks and a vast peneplain formed throughout the Middle East [Garfunkel, 1988]. In places, the eroded top of the igneous complex of Timna is unconformably overlain by a Cambrian sedimentary sequence. From the Early Cambrian until middle Cenozoic the area generally behaved as a stable platform.

The platform stage was interrupted by early Cretaceous intraplate hot spot volcanism known in Israel from outcrops and boreholes [Garfunkel, 1988]. The southernmost identified outcrop of lower Cretaceous volcanics is a 250 m² basaltic plug located about 2 km north of Mount Timna, and there are a few occurrences of basaltic pyroclastic rocks nearby. Magnetometer surveys indicate that more such buried bodies are located in the vicinity [Beyth and Segev, 1983; Segev et al., 1992].

Right-lateral motion on the E-W trending Negev-Sinai shear belt, including the Themed fault located 5 km south of Mount Timna (Figure 1b), dextrally offsets 20-22 Ma dikes. The shear belt was sinistrally displaced by the Dead Sea transform [Eyal et al., 1981]. Hydrothermal mineralization is common along segments of the shear belt. The predominance of E-W Precambrian faults near Elat and in southeast Sinai led Garfunkel [1970] to suggest that the Themed fault is a rejuvenated Precambrian fault.

In middle Tertiary time, Arabia started to drift away from Africa as new plate boundaries formed, eliminating the Tethys ocean floor to the north, eventually colliding with the Eurasian continent in the late Miocene. Left lateral motion along the Dead Sea transform started in middle Miocene time. This offset amounts to ~105 km of which about two thirds had taken place in the Miocene [Garfunkel, 1988; Quennell, 1956]. Uplifting and erosion, accompanied by rift faulting and magmatism, commenced in Sinai about 26.6±3 Ma and continued for most of the Miocene [Kohn and Eyal, 1981]. In Israel the main phase of uplifting was younger, occurring during the middle to late Miocene. Faulted terraces and seismic activity indicate that left-lateral motion is continuing along the Dead Sea transform [Garfunkel et al., 1981].

Cretaceous magmatism and Cenozoic rifting were accompanied by hydrothermal activity and other alteration processes that are potential modifiers of the primary thermoremanent magnetizations (TRM) in the Precambrian rocks. A number of such processes have been documented on Mount Timna and in its vicinity. These include strongly altered basement (gabbroic to dioritic) rocks, with a typical greenish hue dubbed "Deshe" (grass, in Hebrew), which form a ~700 m² depression in the center of Mount Timna [Bentor, 1961; Beyth, 1987a]. The same altered rocks envelop small fresh outcrops of exfoliated gabbro and diorite in the northern part of Mount Timna. Hydrothermal quartz, barite, and calcite in veins cut all the igneous rocks of Mount Timna [Bar-Matthews and Matthews, 1990; Zlatkin and Würzburg, 1957].

A sandy facies of the Lower Cambrian Timna formation enriched with manganese, copper, and uranium is found along fault lines related to the Dead Sea transform. These faults enabled circulation of fluids that leached out the dolomite from the Timna formation [Beyth, 1987b; Segev and Sass, 1989]. Uranium was also leached out of manganese nodules, and the mineralogy of the nodules has been changed by alteration processes [Bar-Matthews, 1986; Bar-Matthews and Matthews, 1990]. Low-temperature geothermal waters that are found in the

modern copper mines of Timna contain a variety of solubles leached out of the host rocks [Beyth et al., 1984].

METHODS

A total of 141 samples from 23 sites of eight igneous rock types on Mount Timna were collected for paleomagnetic analyses. The gabbro was sampled at seven sites, 50-200 m apart, each one on a separate, boulderlike, exfoliated outcrop. The dikes were chosen so as to include a variety of orientations and compositions. The sampling sites included fresh looking outcrops except for one site of altered gabbro ("Deshe") which was sampled in order to compare an obviously altered rock with the apparently fresh outcrops of the other rock types. All the samples were drilled in the field with a portable drill; orientation of the cores was determined with a sun compass. The friable Deshe was sampled with oriented plastic capsules. The core samples were sliced into 2.5-cm-long specimens to achieve equidimensionality. Several samples were sliced into two specimens, one for alternating field (AF) and the other for thermal treatment. Thin sections were made from cores taken at each sampling site for mineralogical examination.

The measurements of remanent magnetizations were made with a three-axis superconducting magnetometer ("2G Enterprises"), equipped with a mounted AF demagnetizer, at the Institute for Petroleum Research and Geophysics in Holon.

The direction (declination inclination) and intensity (J) of the natural remanent magnetization (NRM) were measured first, and then the specimen was subjected to stepwise demagnetization by peak alternating fields of increasing intensity, starting with 5 or 10 mT and going up to 80-100 mT in 5- or 10-mT increments. Selected specimens were subjected to thermal cleaning by heating to 690°C in steps of 50°C-100°C in a field-free environment. An AF of 5 mT was applied to the specimens before measurement to remove possible magnetizations acquired during transferral from the oven to the field-free container where they were left to cool down. The remanent magnetization was measured after every demagnetization step.

It is assumed that no tectonic corrections to the data are required since the Precambrian dikes are vertical throughout Mount Timna and relics of Cambrian sediments on top of Mount Timna are essentially horizontal, ruling out post-Cambrian tectonic tilting.

Standard orthogonal vector plots [Zijderveld, 1967] are used to illustrate the direction and intensity (J) of the remanent magnetic vector before demagnetization (the NRM) and as demagnetization proceeds (Figure 2). The vector directions were defined as the linear sections that approach the origin and pass a 2° linearity test. The components of low coercivity or unblocking temperatures were resolved by vector subtraction. Stereographic projections are used for comparing vector directions.

Each sampling site includes six individual samples whose magnetic vectors are averaged to give the site mean inclination and declination. The mean direction of all the sites in the same rock unit is taken as the characteristic direction of that unit. The precision parameter (k) and angular radius of the 95% confidence circle (α_{95}) are calculated using Fisher's [1953] statistics.

Electron microprobe analyses of the ore minerals were made on carbon-coated, finely polished thin sections of all rock types. The analyses were performed with a Jeol JXA

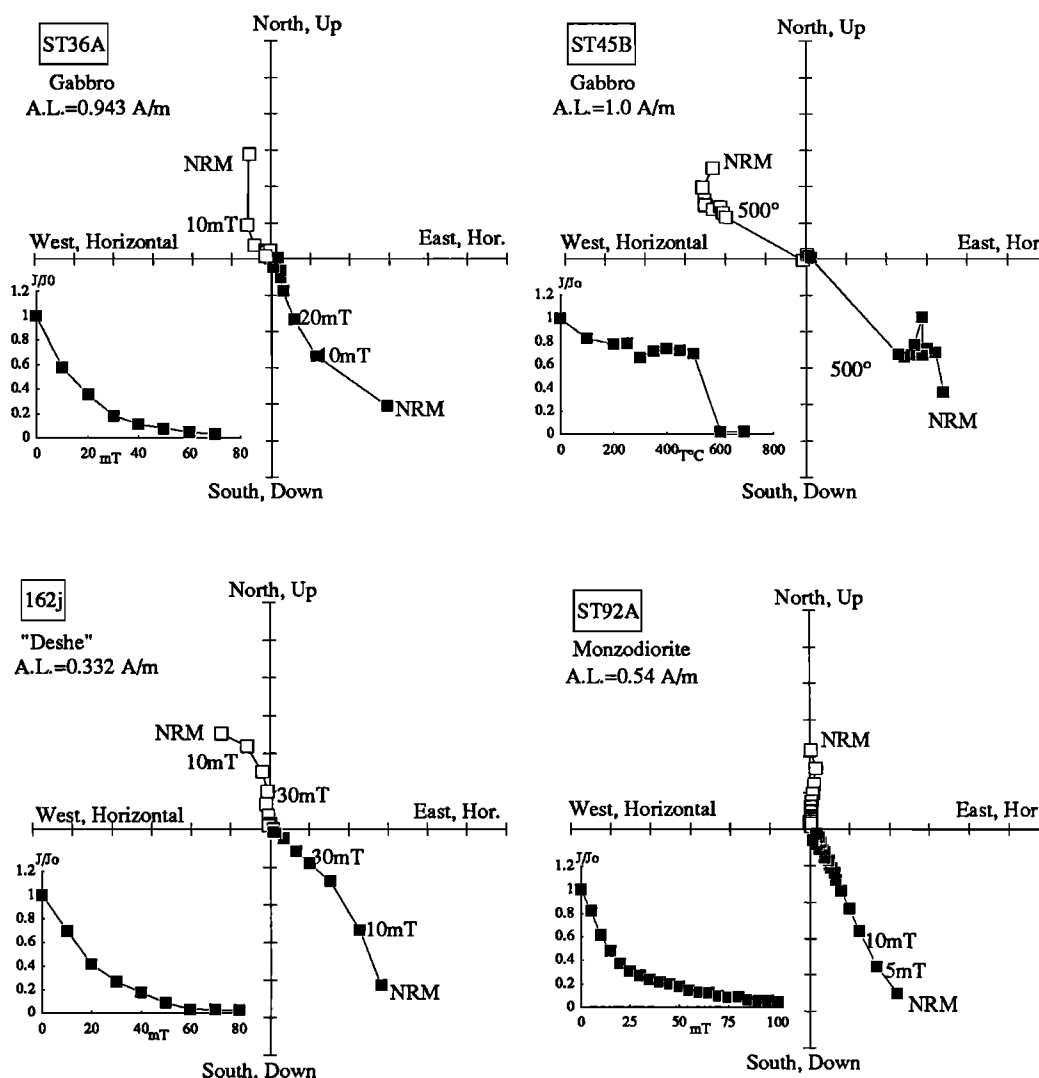


Fig. 2. Orthogonal vector plots of representative samples. Solid squares denote true inclinations, measured clockwise from the horizontal axis. Open squares are declinations, measured clockwise from the north axis. The inset plots in the lower left quad show the normalized intensity (J/J_0) as a function of the alternating field in millitesla or temperature in degrees Celsius. A.L., axis length. See text for discussion.

8600/Tracor System II automated electron probe microanalyzer equipped with four wavelength dispersion spectrometers (WDS) and Tracor Northern energy dispersion spectrometers (EDS) using a 20-keV, 10-nA electron beam. The ore minerals were qualitatively identified by their EDS spectrum and then quantitatively analyzed by WDS.

The texture and distribution of the phases were studied by computer-generated X ray mapping which was done with a combination of WDS and EDS. Each spectrometer was set to a particular element (Fe, Ti, Ca, and Si), and an image was constructed by measurements of the X ray intensity during slow scanning with the beam. Selected phenomena were recorded in photographs of backscattered electron images (Figure 3).

RESULTS

The mineralogical and petrographical results are summarized in Table 1 and Figure 3. Mean destructive field and magnetic moment density are given in Table 1 and the paleomagnetic results are given in Table 2 and Figures 2 and 4.

All rocks studied show varying degrees of replacement and alteration of major mineral constituents to clays, sericite, serpentine, and chlorite (Table 1). Similarly, all the rocks contain secondary magnetic minerals, mainly goethite, hematite, and some magnetite. The goethite appears as cryptocrystalline aggregates; the hematite is xenomorphic and is recognizable in polarizing microscope by its distinct reddish hue. The secondary magnetite grains are xenomorphic and usually smaller than the primary idiomorphic grains. Exsolutions of Ti-magnetite are also observed. Most of the alteration products of both major constituents and of the magnetic minerals usually form in processes involving oxidation and hydration which are typical of hydrothermal alteration and weathering of the igneous minerals.

A summary of the characteristic directions of magnetization (Table 2 and Figure 4) shows that a group of four rock types (Deshe, monzodiorite, the dikes, and the quartz monzodiorite, units 2, 3, 5, 6, 7, and 8 in Table 2) have a north trending declination and an average inclination of 41° . The average direction of the alkali granite is $343^\circ/14^\circ$, $\alpha_{95}=22^\circ$, one site of

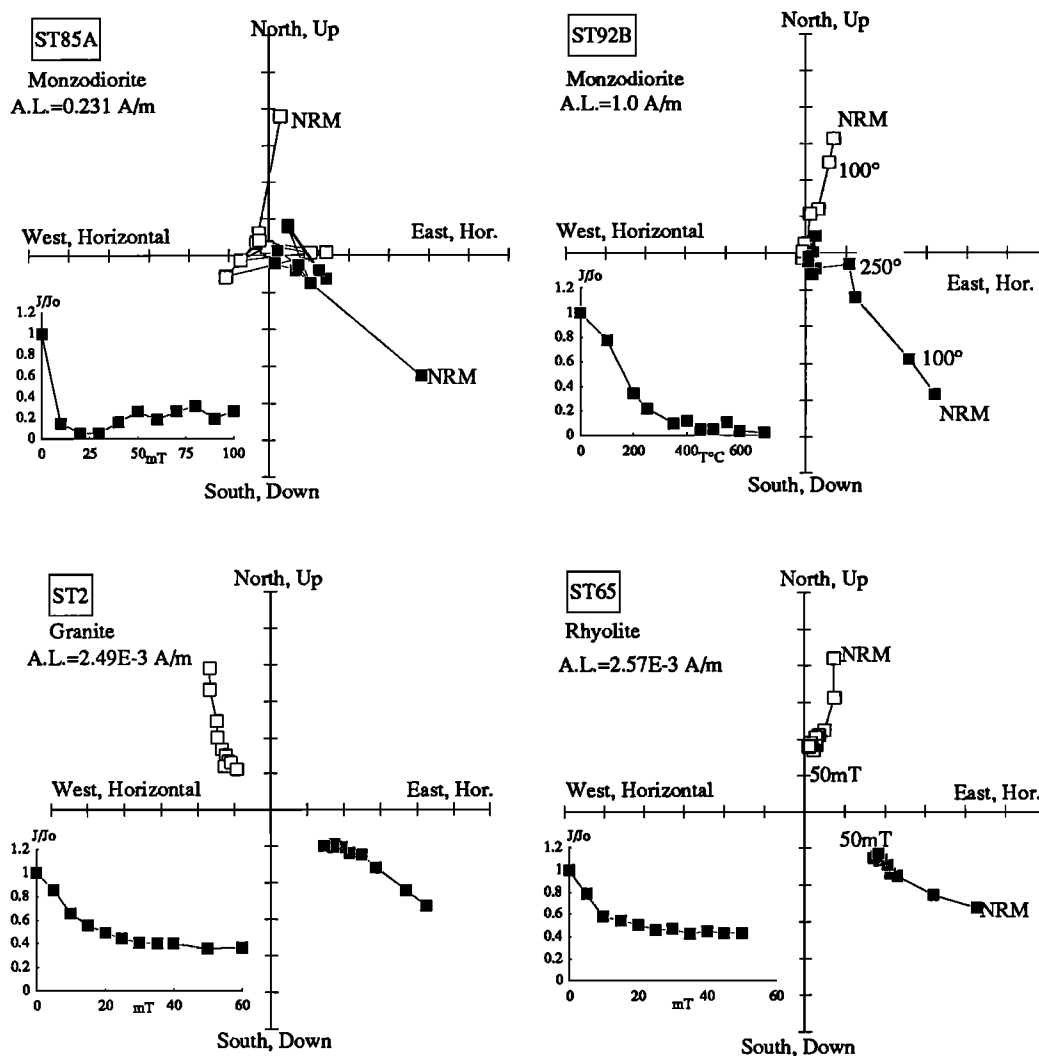


Fig. 2. (continued)

a dolerite dike gives $318^\circ/0^\circ$, $\alpha_{95}=2^\circ$, and the average of seven gabbro sites is $303^\circ/56^\circ$, $\alpha_{95}=6^\circ$.

In Figure 4 our results are compared with those of previous workers who studied Lower Cambrian sediments [Ron and Kolodny, 1985], Lower Cretaceous basalts [Ron and Baer, 1988], and Miocene to Recent basalts and sediments [Ron *et al.*, 1984]. On the basis of these studies, the expected magnetic field direction for the Lower Cambrian is (D/I) $315^\circ/9^\circ$, $\alpha_{95}=17^\circ$, for the Lower Cretaceous $340^\circ/12^\circ$, $\alpha_{95}=7^\circ$, for the Miocene $005^\circ/45^\circ$, $\alpha_{95}=3^\circ$ and for the present-day $000^\circ/47^\circ$ (Figure 4).

Petrologic Evidence for Alteration of Magnetic Minerals

The most critical paleomagnetic issue is whether or not the original magnetic mineral assemblage was modified along with the alteration of the major constituents. Modification of the magnetic minerals would result in acquisition of chemical remanent magnetization (CRM). Detailed electron probe and petrographical studies reveal a number of phenomena that are indicative of alteration of the magnetic minerals of the Mount Timna intrusives and the formation of secondary minerals:

1. Magnetite appears inside serpentine as an alteration product of the olivine in the gabbro (Figure 3a).

Serpentinization results in a typical aggregate of fine-grained serpentine with disseminated Fe-oxides. Serpentine and magnetite commonly replace Mg-olivine and Ca-poor orthopyroxene in basic rocks. Since magnetite is the principal carrier of the magnetization in the gabbro, it appears that the acquisition of its magnetization occurred as the serpentine and associated magnetite crystallized. The wide variety of conditions in which serpentinization occurs makes it difficult to establish reliable criteria for the time and setting of serpentinization. Beyth [1987a] noted the possibility that hydrothermal activity of the Dead Sea rift waters caused the serpentinization in Timna.

2. Single Ti-magnetite crystals are altered into exsolved Fe and Ti oxides. The alteration, as opposed to exsolution, appears in back-scattered electron images (BSE) as an irregular pattern of darker Ti oxides and lighter Fe oxides. Oxidation of Ti-magnetite at low temperatures (<200 - 250°C) leads to the formation of Ti-hematite which ultimately inverts to hematite with some TiO_2 [Ramdohr, 1969].

3. Hematite is present as a secondary mineral in andesite, rhyolite, and western dolerite dikes and in the alkali granite and the quartz-monzodiorite plutons. Hematite is rare in igneous rocks, especially in those of intermediate and mafic composition, and its presence is almost always a product of

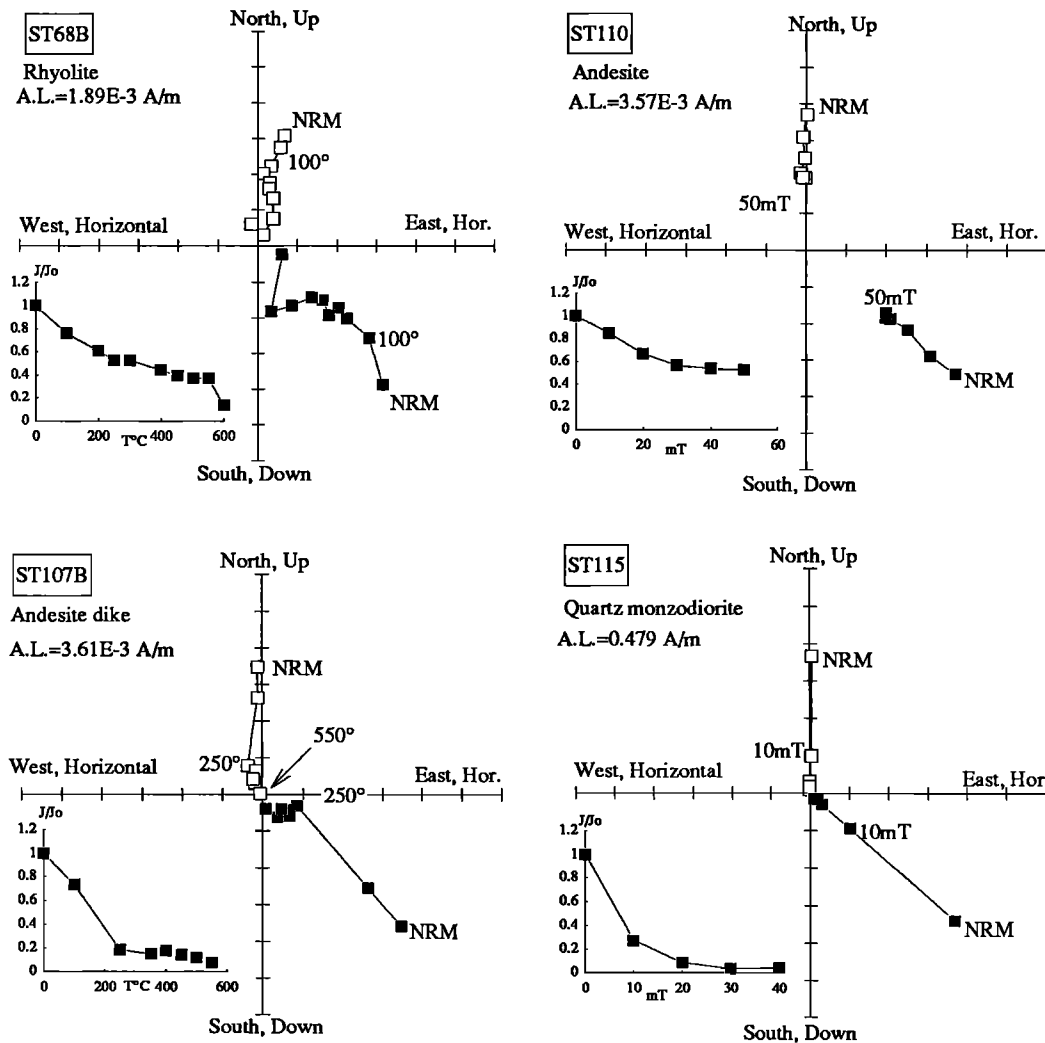


Fig. 2. (continued)

alteration [Best, 1982]. Hematite was identified by the electron probe, by its reddish hue in polarizing microscope, and by its high magnetic coercivity. It could have been formed in the subject rocks by oxidation of magnetite [Ramdohr, 1969] or dehydration of goethite.

4. Sphene (CaTiSiO_5) is replaced by Fe-Ti oxides and secondary overgrowths of sphene on the same grains. Sphene is known in hypabyssal suites as a product of autometasomatism by reaction of residual liquids with early formed Fe-Ti oxides [Haggerty, 1976]. However, the appearance of sphene in the monzodiorite of Mount Timna as idiomorphic, partly replaced grains and as irregular overgrowths suggests a formation by hydrothermal reactions.

5. Hydrous phases are present as replacements of Fe-bearing minerals. A typical example is an irregular aggregate of cryptocrystalline goethite (Figure 3b). Goethite, which had been reported as a carrier of CRM [Strangway et al., 1968], is present in all the dikes. On heating to about 200°–400°C, goethite dehydrates to hematite.

6. There are veins and vesicles of calcite, dolomite, barite, and manganese within the ore grains (Figure 3c). These soluble phases are indicative of water percolation through fractures, after crystallization of the magmas.

7. Magnetite grains in the altered gabbro ("Deshe") are

equidimensional, whereas in the gabbro protolith they are acicular. The magnetite in the Deshe is either a product of precipitation from Fe-bearing fluids associated with the alteration of the gabbro or fragments of the original magnetite. In both cases, magnetization would have been acquired contemporaneously with the alteration, either as the grains nucleated and grew or perhaps as the fragments were reoriented while the "Deshe" was undergoing hydration.

The observations presented above show that all the intrusive rocks studied contain secondary oxidized and hydrated magnetic minerals. Some of the idiomorphic magnetite present in all the rocks that show no signs of alteration may be primary. An unequivocal distinction between primary and alteration-derived magnetite cannot be made in the present study. It is assumed that idiomorphic magnetite, present in small quantities in all rock types with no signs of alteration (or in association with an altered paragenesis), is primary.

Other phases of primary origin include chromite in the gabbro (Figure 3a) and Ti-magnetite in the monzodiorite, quartz monzodiorite, and dolerite.

Paleomagnetic Results

The alteration phenomena and the identification of secondary magnetic minerals make it very probable that CRM

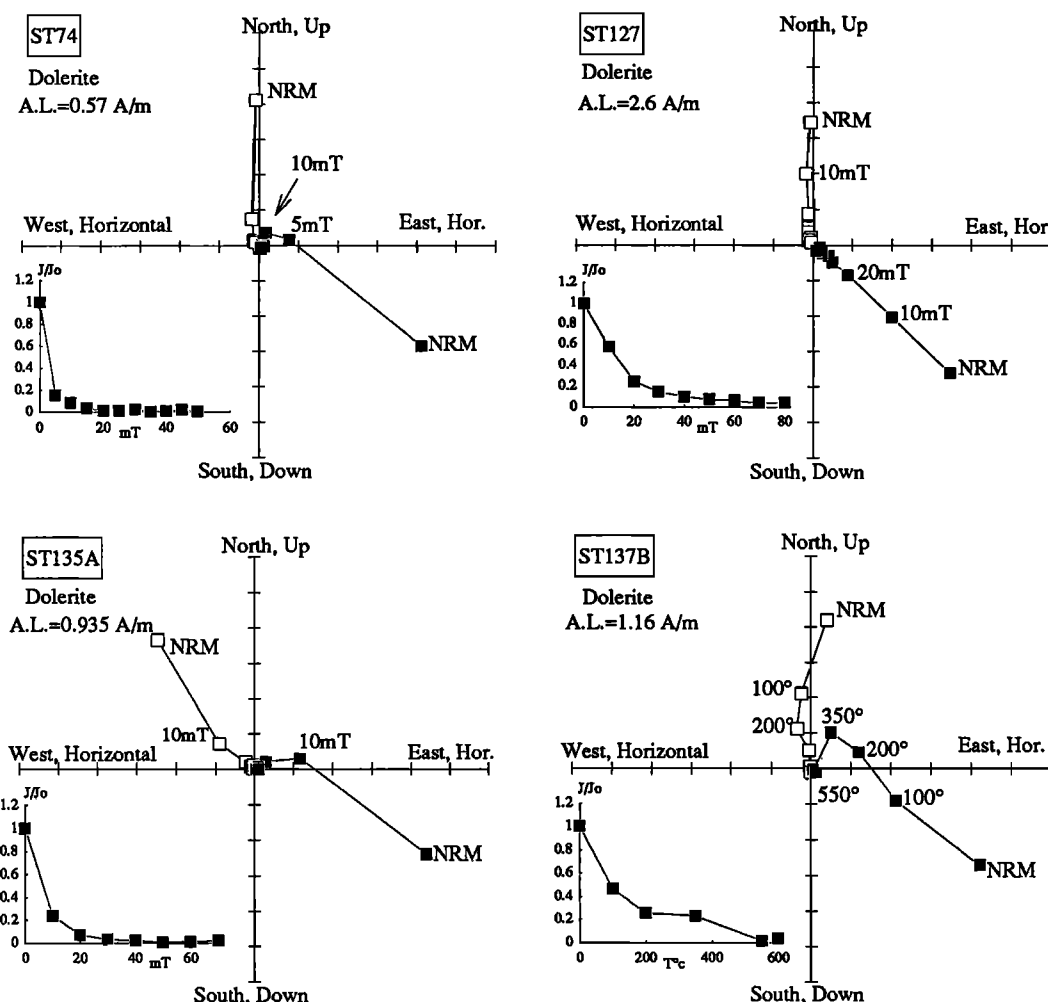


Fig. 2. (continued)

was acquired by many of the studied rocks. In this section the paleomagnetic properties of the rocks are explored in order to test their compatibility with the mineralogy.

The paleomagnetic measurements summarized in Table 2 and Figures 3 and 4 are described and compared with Phanerozoic field directions in the following section:

Gabbro. Most samples show a viscous overprint of either a reverse or normal recent field which is typically removed by 10–15 mT. The characteristic direction is $303^\circ/56^\circ$, $\alpha_{95}=6^\circ$ (Figure 2, ST36A). The thermal demagnetization curve is typical of magnetite held magnetization, with a maximum unblocking temperature of 575°C (Figure 2, ST45B). Chromite, a ferrimagnetic mineral, is also an efficient carrier of stable remanence [Refai et al., 1989] but much weaker than magnetite.

"Deshe" (altered gabbro). One component is removed by 10–20-mT field and the rest of the magnetization is completely removed by 60 mT. The curve is typical of magnetite-held magnetization. The direction of the low-coercivity component is similar to the gabbro. The higher-coercivity component ($353^\circ/48^\circ$, $\alpha_{95}=7^\circ$) is similar to the subrecent direction, between $005^\circ/47^\circ$, $\alpha_{95}=3^\circ$ in the Miocene and $360^\circ/45^\circ$ at Present (Figure 2, 162J).

Monzodiorite. The NRM is mostly composed of one stable vector (Figure 2, ST92A), but in a few samples it is very unstable (Figure 2, ST85A). Thermal demagnetization removed

70–80% of the intensity by 200°C (Figure 2: ST92B), which may be attributed to fine-grained goethite, observed in small amounts in the samples. The rest of the magnetization is held by Ti-magnetite. The field direction ($356^\circ/42^\circ$, $\alpha_{95}=5^\circ$) is similar to the subrecent.

Alkali granite. The paleomagnetic results are too variable to interpret coherently. Of 13 samples obtained (two sites), three have a very unstable vector, four were only partly cleaned by AF treatment, a behavior typical of hematite (Figure 2: ST2), and six exhibited a magnetite-held stable magnetization. The average direction of 10 samples is $343^\circ/14^\circ$, $\alpha_{95}=22^\circ$. Figure 4 shows that this is very close to the Lower Cretaceous field direction, $340^\circ/12^\circ$, $\alpha_{95}=7^\circ$ [Ron and Baer, 1988].

Rhyolite dikes. Between 20% and 80% of the NRM intensity is removed by AF (Figure 2, ST65). Because large magnetite grains are not observed in the samples, this is taken to indicate that the magnetization is held by magnetite with variable amounts of hematite and goethite. Eighty percent of the NRM intensity is removed by AF demagnetization where the major mineral is magnetite with some hematite and goethite; 20% is removed where the major mineral is hematite and the magnetite is a minor constituent. The field direction ($010^\circ/38^\circ$) is similar to the Miocene. In four samples, a present-day field component comprising about 50% of the total NRM intensity was removed upon heating up to 250°C .

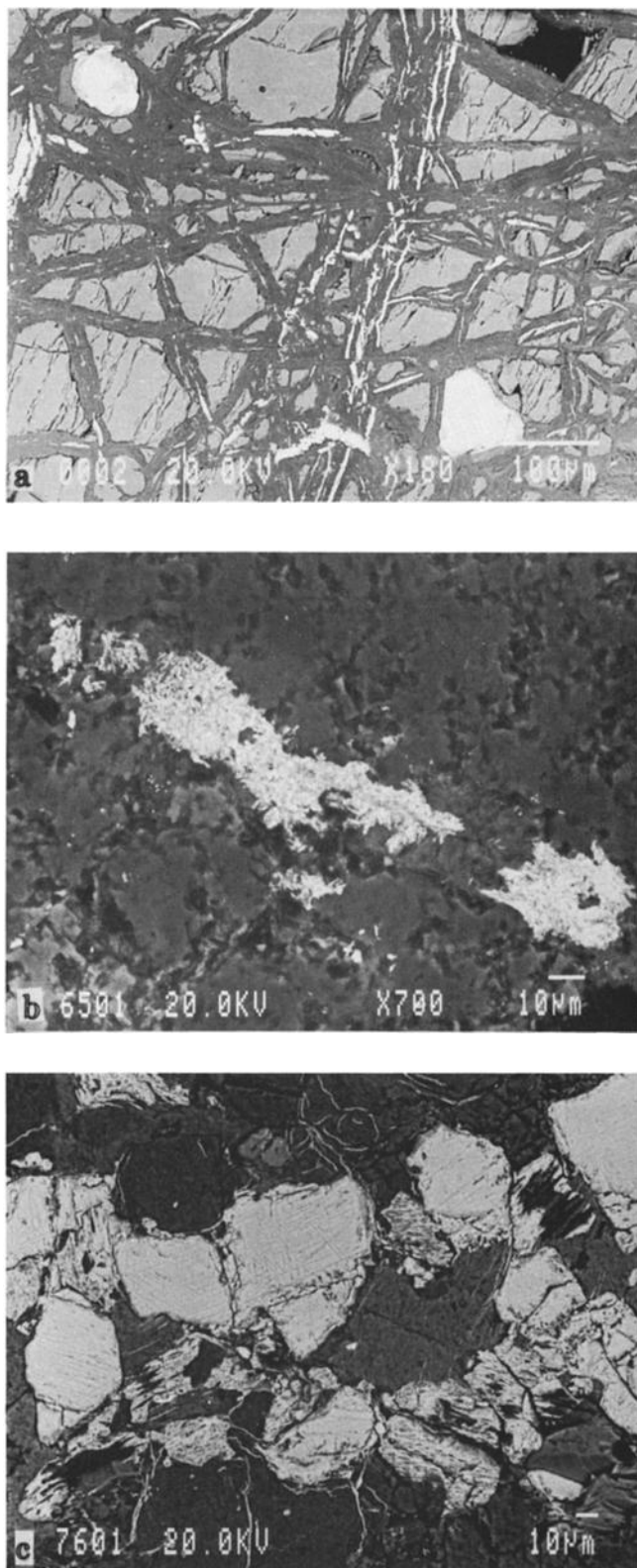


Fig. 3. Backscattered electron images of common alteration phenomenon: (a) Gabbro, acicular magnetite surrounded by serpentine. Large white grains are chromite. (b) Rhyolite, cryptocrystalline aggregate of hydrous Fe-oxide, most probably goethite. (c) Dolerite, exsolution in Ti-magnetite grains. Silicate minerals are replaced by Fe-oxides leaving residual quartz cores. In both the quartz and the Fe-oxides the original cleavage of the silicate mineral is conspicuous. White veinlets are filled with barite.

Between 550° and 600°C, about 40% more of the NRM intensity was removed (Figure 2, ST68B); this portion was carried by magnetite with a horizontal inclination and north trending declination. The remaining 10% of the NRM intensity was carried by hematite. Some of the magnetite is probably primary, and the horizontal inclination may therefore be attributed to an original TRM.

Andesite dikes. The NRM is composed of at least two vectors residing in part in high-coercivity minerals, which do not respond to AF demagnetization. After removal of 30-50% of the NRM by 40 mT, the direction of the remanent field (003°/36°) is similar to the subrecent direction (Figure 2, ST110). Thermal demagnetization (Figure 2, ST107B) is typical of goethite and minor magnetite-held remanence (60-90% loss of the intensity upon heating to 300°C). The high T_b component (>250°C) occasionally has a shallow inclination and NNW declination (Figure 2, ST107B), which is similar to the Early Cambrian direction. This component is probably carried by magnetite grains which were not altered to goethite and may therefore be attributed to an original TRM. In several samples the intensity decreased first by 25% between 250° and 300°C and again between 400° and 550°C, typical of mainly magnetite- and some goethite-held magnetizations. The presence of both is also confirmed by electron microprobe analyses. The shallow inclinations are present in these samples too, but the declinations vary between NW and NE.

Quartz monzodiorite. The behavior during AF treatment is very uniform: the vector is stable and always completely removed by a 30 mT field, indicative of magnetite. The observed direction (360°/42°) is similar to the recent field direction (Figure 2, ST115).

Dolerite dikes. Two NW striking dikes were sampled. In both, the NRM direction is similar to the subrecent direction (Figure 2, ST74) and after 5 to 10 mT AF treatment, a reverse field direction is isolated. The higher-coercivity component has a shallow inclination.

In the eastern dike, seven samples of one site (site 8 in Figure 1c) show a stable, one-component, magnetite-held component with a direction similar to the subrecent field (38°/356°) with or without a very soft overprint (Figure 2, ST127). The maximum demagnetization field is 50-60 mT. The magnetite in these samples is secondary (Figure 3c), and only minor amounts of fine grained hematite and goethite are present. In six samples of the second site in the same dike (site 9 in Figure 1c), about 80% of the NRM is a viscous overprint (Figure 2, ST135A) typically removed by 5-10 mT. The direction of the overprint is similar to the subrecent. The higher-coercivity component is removed completely by 25-30 mT and its direction (318°/0°) is similar to the expected Early Cambrian field [Ron and Kolodny, 1985]. Thermal treatment (Figure 2, ST137B) removes ~80% of the magnetization upon heating to 200°C and the rest by 550°C. The low-temperature subrecent component is interpreted as a goethite held magnetization and the higher temperature is held by magnetite. The high-coercivity component is interpreted as unaltered magnetite that preserves the primary magnetization. All samples from the western dike (site 10 in Figure 1c) contain large amounts of hematite and goethite and were unstably magnetized.

In summary, a group of four rock types (altered gabbro "Deshe," monzodiorites, most of the dikes, and quartz monzonites) has north trending declinations and an average inclination of 41°, which is similar to the direction of the field

TABLE 1. Magnetic Mineralogy, Alteration Phenomena, Mean Destructive Field, and Natural Remanent Magnetic Moment per Unit Mass J_o

Rock Unit	Locality (Figure 1c)	Magnetic Minerals	Alteration Phenomena	MDF, mT	J_o , A m ² kg ⁻¹
Gabbro	1	magnetite, chromite	olivines→serpentine and magnetite (Figure 3a)	13-18	$10^{-3} - 10^{-4}$
Altered gabbro	2	magnetite	complete serpentinization, abundant clays and chlorites	15-18	10^{-4}
Monzodiorite	3	magnetite, Ti-haematite, goethite	sericite, clays, Ti-magnetites→TiO ₂ +Fe oxides, sphene→Fe+Ti oxides, magnetite→goethite	6-10	$10^{-4} - 10^{-5}$
Alkali granite	4	haematite, Ti-haematite, magnetite	minor sericite, partial magnetite→haematite	8-18	$10^{-6} - 10^{-7}$
Andesite dikes	5	magnetite, Ti-haematite, goethite, haematite	some sericite, abundant clays, vesicles of barite and carbonate, magnetite→goethite and haematite		$10^{-4} - 10^{-6}$
Rhyolite dikes	6	magnetite, goethite, haematite	sericite, abundant clays, magnetite→goethite and haematite (Figure 3b)		10^{-6}
Quartz monzodiorite	7	magnetite, Mn bearing Ti-haematite	silicates→chlorite, clays and magnetite, veins of barite and carbonate, exsolution of Ti-magnetite	7	10^{-4}
Dolerite dike east	8 and 9	magnetite, Ti-magnetite, goethite	silicates→chlorite, clays and magnetite, veins and vesicles of barite and carbonate, magnetite→goethite	5-10	$10^{-3} - 10^{-4}$
Dolerite dike west	10	magnetite, Ti-magnetite, goethite, haematite	silicates→chlorite, clays and magnetite, veins and vesicles of barite and carbonate (Figure 3c), magnetite→goethite and some haematite	5-10	$10^{-3} - 10^{-4}$

since the Miocene [Piper, 1988; Ron *et al.*, 1984]. The alkali granite direction (343°/14°) resembles that of the Early Cretaceous, 340°/12°, $\alpha_{95}=7^\circ$ [Ron and Baer, 1988] and one dolerite site has a direction (318°/0°) similar to that of the Early Cambrian [Ron and Kolodny, 1985]. The gabbro (303°/56°) has no known comparable direction. The gabbro samples were taken from several outcrops adjacent to monzodiorite intrusions (Sits 1 and 3 in Figure 1c). The irregular shape of the contact and the absence of faults indicate that the gabbro could not have rotated alone. We therefore rule out the possibility that the exceptional field direction of the gabbro results from rotation.

DISCUSSION

One possible alternative to CRM is magnetization during continental drift; that is, the "subrecent" direction is primary and was acquired when the Precambrian location of Timna was similar to the present. This is not considered viable: the different directions cannot reflect continental drift as this implies an improbable apparent polar wander path. The pole would have to return to the same position intermittently at the time of emplacement of the monzodiorite, the ENE striking andesitic and composite dikes, the quartz-monzodiorite, and the NW striking doleritic dikes; at time of the alteration of gabbro

TABLE 2. Results of Paleomagnetic Measurements of Igneous Rocks in Mount Timna, 29.8°N, 34.9°E

No.	Rock Unit	Sites	N	D	I	R	k	α_{95}	Pole	δp	δm
1	Gabbro	7	43	303°	56°	0.930	14.4	6°	328.9°E, 42.5°N	8.8	8.6
2	Altered gabbro (Deshe)	1	10	353°	48°	0.973	37.1	7°	299.6°E, 83.9°N	11.5	9.1
3	Monzodiorite	4	24	356°	42°	0.983	57.3	5°	248.5°E, 83.4°N	8.7	6.1
4	Alkali granite	2	13	343°	14°	0.805	5.1	22°	253.4°E, 62.2°N	43.5	22.5
5	Andesite dikes	4	24	003°	36°	0.998	402	3°	198.8°E, 79.8°N	5.5	3.5
6	Rhyolite dikes	2	10	005°	42°	0.990	101	5°	175.0°E, 82.9°N	8.7	6.1
7	Quartz monzodiorite	1	4	360°	42°	0.999	671	3°	214.9°E, 84.4°N	5.2	3.7
8	Dolerite dike east 1	1	7	356°	38°	0.992	129	5°	238.9°E, 80.8°N	9.0	5.9
9	Dolerite dike east 2	1	6	318°	0°	0.999	1876	2°	276.0°E, 40.2°N	4.0	2.0
10	Dolerite dike west*	1	4								

* Very unstable, omitted

Rock units are detailed in order of descending age, determined by field relations [Shpitzer *et al.*, 1991]. The directions refer to the stable component. R is the length of the resultant unit vector (maximum 1, when all the vector directions are identical). k is the precision parameter, $k=N/[N(1-R)]$, where N is the number of vectors. α_{95} is the angular radius of the 95% circle of confidence, $\alpha_{95}=140/(kN)^{0.5}$, δp and δm are the half axes of the 95% oval of confidence of the poles (latitude and longitude).

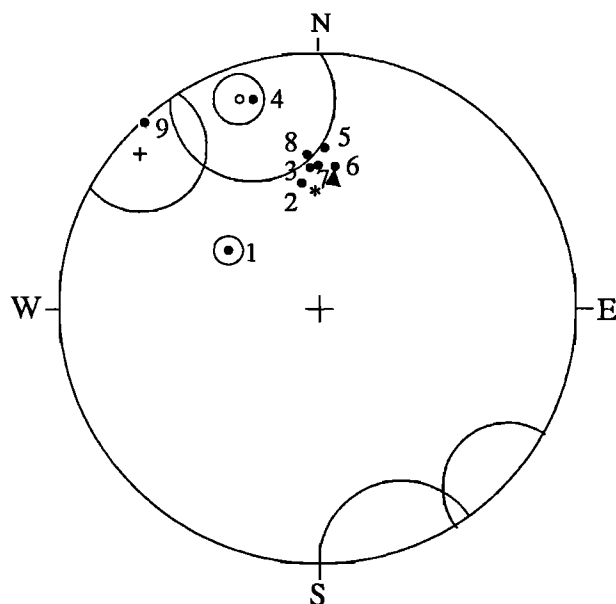


Fig. 4. Equal-angle projection of paleomagnetic field directions (inclinations and declinations) of igneous rocks of Mount Timna compared with several Phanerozoic directions. Solid circles, this study, numbers refer to Table 2; triangle, Miocene field direction 005°/45°, $\alpha_{95}=3^\circ$ [Ron et al., 1984]; star, present field 000°/47°, open circle, Lower Cretaceous field 340°/12° $\alpha_{95}=7^\circ$ [Ron and Baer, 1988]; cross, Lower Cambrian field direction 315°/9° $\alpha_{95}=17^\circ$ [Ron and Kolodny, 1985]. Small circles mark the α_{95} of the gabbro (1), alkali granite (4), Lower Cretaceous and Lower Cambrian expected directions. The α_{95} of 3° of the Miocene is too small to plot here.

to Deshe; and finally in the Neogene. Departures from this position would have taken place when the gabbro and the alkali-granite were emplaced and between Cambrian and Neogene times.

Thermal resetting of the magnetization was also unlikely to occur because the blocking temperatures (T_b) of most of the primary magnetic minerals are above 400°C. This range of temperatures was never reached beneath the thin cover (<2 km) of the Phanerozoic sediments, even if an anomalously high thermal gradient is assumed. The low T_b hydrous phases (e.g. goethite, $T_b=110^\circ\text{--}120^\circ\text{C}$) are secondary minerals. Heating due to the sparse Cretaceous volcanism is not likely to have affected a broad area and would have resulted in the characteristic Early Cretaceous field direction of 340°/12° [Ron and Baer, 1988]. The direction of the granite, 343°/14°; $\alpha_{95}=22^\circ$, is similar to the Early Cretaceous direction but the absence of similar directions in other sites hints that this is a spatially restricted resetting.

The analysis of the paleomagnetic field directions is thus consistent with our earlier observation that resetting of the magnetization during alteration of the original magnetic minerals and the formation of secondary magnetic minerals is the most probable process involved in resetting of the primary magnetization.

Bearing in mind the mineralogical observations presented earlier, the following criteria support the interpretation that chemical alteration is the mechanism of remanence acquisition in Mount Timna:

1. Hematite and goethite, which are secondary minerals, carry part and often the entire magnetization of the samples with the subrecent field direction. The other directions in the same rocks are carried by magnetite, which is usually a primary mineral.

2. A number of samples are unstably magnetized, a phenomenon which is attributed to alteration of the magnetic carriers [Nagata, 1961].

3. The magnetic field direction of the Deshe is different from its protolith but similar to the subrecent field. The Deshe is an obvious case of hydrothermal alteration and was sampled as a reference for unaltered rocks. This result implies that massive alteration occurred in subrecent time.

4. The "subrecent" direction appears as both an overprint (implying partial alteration) and as the sole stable vector (complete alteration) in the dolerite, rhyolite, and andesite dikes.

It is concluded that rocks having magnetic fields with north trending declinations and inclinations of about 40° acquired them when secondary magnetic minerals formed as a result of alteration processes in the subrecent field.

GEOLOGIC AND TECTONIC IMPLICATIONS

The virtual absence of reversals in the rocks that acquired CRM implies that the process probably occurred within a time interval not longer than ~1 m.y., the maximum duration of normal polarities since the Oligocene. The hydrothermal activity has been going on since the onset of faulting in middle Miocene time, but the alteration processes in the rocks studied here probably ended after less than 1 m.y.

It is assumed that hydrothermal alteration in the basement rocks occurred beneath the sedimentary cover, before the uplift and erosion of the area, in the early stages of the Dead Sea transform activity. The alternative possibility of recent alteration by weathering at the surface is less likely, given the present arid desert conditions. The north trending declinations therefore imply that Mount Timna has not rotated about a vertical axis since the early stage of the Dead Sea transform. The presence of goethite puts constraints on the thermal regime subsequent to its formation because it dehydrates to hematite at 200°–400°C [Ramdohr, 1969].

The margins of the transform in the area to the south of Timna are deformed by sinistral movement along N-S striking faults. A 20° northward deflection of the strike of the eastern segment of the Themed fault points to counterclockwise rotation of the area (Figure 1b). A structural analysis [Garfunkel, 1970] concluded that the rotation is expected to decrease northward in the direction of Timna because the deformation is taken up by E-W striking structures such as a syncline and reverse faults. The north trending declinations in Timna are therefore consistent with the structural analysis and provide an independent support for Garfunkel's conclusions.

The field direction of the gabbro (303°/56°), in which the magnetite occurs as a secondary mineral enclosed in serpentinized olivines, differs from the subrecent. It presumably acquired its magnetization during the serpentinization, a process whose time and physicochemical conditions are yet to be determined.

When the intrusive rocks of Timna formed in the late Precambrian, the Arabo Nubian Massif, including Timna, was already a part of Africa [Bentor, 1985]; therefore the pole positions of the studied rocks should be compared with those from Africa. However, the large scatter of pole positions determined from late Precambrian rocks of Africa [Kröner et al., 1980; Piper, 1988; Sallomy and Krs, 1980; Saradeth et al., 1989] makes it impossible to compare the African data with those from Timna. The calculated virtual geomagnetic pole for the Timna rocks with subrecent field directions is at 223°E, 84°N. It is incompatible with the Precambrian position

of Africa suggested by various authors [Burrett *et al.*, 1990; Piper, 1987; Scotese and Barrett, 1990] on the basis of biogeographic, climatically sensitive lithofacies and paleomagnetic data.

The shallow inclination component of the rhyolite, andesite, and dolerite dikes (0° - 10°) is held by magnetite and may be interpreted as the remnants of the original thermoremanent magnetization. If this interpretation is correct it implies a near-equatorial location of the region in late Precambrian to Early Cambrian time. Support for the near-equatorial location is provided by red clays that are preserved below the Cambrian sediments in Timna and the nature of the weathering of the igneous rocks below the infra-Cambrian peneplain, both are typical of a tropical climate [Garfunkel, 1980]. However, shallow inclinations are observed in only a few samples, and therefore this conclusion is tentative.

CONCLUSIONS

A major group of rocks in Mount Timna acquired CRM in the Miocene due to alteration caused by rift-related hydrothermal activity. The main process was hydration and oxidation of the original magnetic minerals. The alteration occurred within a time interval not longer than 1 m.y., as is evident by the absence of reversals in the rocks that acquired CRM. The north trending declinations imply that Mount Timna has not rotated about a vertical axis since the early stage of the Dead Sea transform activity. This conclusion confirms a structural analysis [Garfunkel, 1970] by an independent method. The subrecent direction of the altered gabbro ("Deshe") indicates that the massive alteration of the gabbro to "Deshe" occurred also in subrecent time. However, in the fresh-looking gabbro (the protolith of the "Deshe") the magnetite is associated with partial serpentinization of olivines and its different magnetic field direction ($303^{\circ}/56^{\circ}$) indicates that this serpentinization occurred at an earlier, as yet undetermined, time. Remnants of original, shallow inclination thermoremanent magnetization apparently support a near equatorial location of the region at the end of the Precambrian.

Acknowledgments. We thank David Shafranek for his invaluable assistance with the electron-microprobe analyses. Ori Gonen, Dalia Marco, Yshai Hoffman, Elon Shamir, and the staff of the Elat Field School of the Society for the Protection of Nature helped in the field work. Critical reviews by Paul Layer, John A. Tarduno, and Jonathan T. Hagstrum have greatly improved the manuscript. The study was supported by the Ministry of Energy, Jerusalem.

REFERENCES

- Baer, G. and M. Beyth, Dike segmentation along preexisting joints and dikes, paper presented at annual meeting, *Isr. Geol. Soc.*, Elat, 1990.
- Bar-Matthews, M., Mineralization of Uranium and other metals in Timna Formation, Timna Valley, *Rep. ZD/115/86*, Geol. Surv. of Israel, Jerusalem 1986.
- Bar-Matthews, M., and A. Matthews, Chemical and stable isotope fractionation in manganese oxide-phosphorite mineralization, Timna Valley, Israel, *Geol. Mag.*, 127, 1-12, 1990.
- Bentor, Y. K., Petrographical outline of the Precambrian in Israel, *Bull. Res. Council. Isr.* 10G, 19-63, 1961.
- Bentor, Y. K., The crustal evolution of the Arabian Nubian Massif with special reference to the Sinai Peninsula, *Precambrian Res.*, 28, 1-70, 1985.
- Best, M. G., *Igneous and Metamorphic Petrology*, 630 pp., W. H. Freeman, New York, 1982.
- Beyth, M., The Precambrian magmatic rocks of Timna Valley, southern Israel, *Precambrian Res.*, 36, 21-38, 1987a.
- Beyth, M., Mineralization related to rift systems: Examples from the the Gulf of Suez and the Dead Sea Rift, *Tectonophysics*, 141, 191-197, 1987b.
- Beyth, M., Mount Timna: Guide to excursion, paper presented at annual meeting, *Isr. Geol. Soc.*, Elat, 1990.
- Beyth, M., and A. Segev, Lower Cretaceous basaltic plug in the Timna Valley, *Isr. J. Earth Sci.*, 32, 165-166, 1983.
- Beyth, M., A. Starinsky, and B. Lazar, Low temperature geothermal waters, Timna, southern Israel, *Geol. Surv. Isr. Curr. Res.*, 1983-1984, 17-20, 1984.
- Burrett, C., J. Long, and B. Stait, Early-middle Palaeozoic biogeography of Asian terranes derived from Gondwana, in Palaeozoic Palaeogeography and Biogeography, *Geol. Soc. Mem. London*, 12, 163-174, 1990.
- Eyal, M., Y. Eyal, Y. Bartov, and G. Steinitz, The tectonic development of the western margin of the Gulf of Elat (Aqaba) rift, *Tectonophysics*, 80, 39-66, 1981.
- Fisher, R. A., Dispersion on a sphere, *Proc. R. Soc. London, Ser. A*, 217, 295-305, 1953.
- Garfunkel, Z., The tectonics of the western margins of the southern Arava, (in Hebrew, English abstract) Ph.D. thesis, 204 pp. Hebrew Univ., Jerusalem, 1970.
- Garfunkel, Z., The pre-Quaternary geology of Israel, in *The Zoogeography of Israel*, edited by Y. Yom-Tov and E. Tchernov, pp. 7-34, W. Junk, Dordrecht, Netherlands, 1988.
- Garfunkel, Z., I. Zak, and R. Freund, Active faulting along the Dead Sea transform (rift), *Tectonophysics*, 80, 1-26, 1981.
- Haggerty, S. E., Opaque mineral oxides in terrestrial igneous rocks, in *Oxide Minerals, Short Course Notes*, edited by D. I. Rumble, pp. Hg101-Hg300, Mineralogical Society of America, Washington D.C., 1976.
- Halpern, M. M., and N. Tristan, Geochronology of the Arabian-Nubian Shield in southern Israel and eastern Sinai, *J. Geol.*, 89, 639-648, 1981.
- Kennedy, W. C., The structural differentiation of Africa in the Pan-African (± 500 million years) tectonic episode *8th Annu. Rep.*, pp. 48-49, Res. Inst. of Afr. Geol., Univ. of Leeds, Leeds, England, 1964.
- Kohn, B. P., and M. Eyal, History of uplift of the crystalline basement of Sinai and its relation to opening of the Red Sea as revealed by fission track dating of apatites, *Earth Planet. Sci. Lett.*, 52, 129-141, 1981.
- Kröner, A., and M. Beyth, Single zircon ages for late Precambrian magmatic rocks of Har Timna, paper presented at Annual Meeting, *Isr. Geol. Soc.*, Elat, 1990.
- Kröner, A., M. O. McWilliams, G. J. B. Gerns, A. B. Reid, and K. E. L. Schalk, Paleomagnetism of late Precambrian to early Paleozoic mixite-bearing formations in Namibia (South West Africa): The Nama group and Blaubecker formations, *Am. J. Sci.*, 280, 942-968, 1980.
- Nagata, T., and K. Kobayashi, Chemical remanent magnetization, in *Rock Magnetism*, edited by T. Nagata, pp. 196-221, Maruzen, Tokyo, 1961.
- Piper, J. D. A., *Palaeomagnetism and the Continental Crust*, 434 pp., Open University Press, Milton Keynes, England, 1987.
- Piper, J. D. A., *Paleomagnetic Database*, 264 pp., Open University Press, Milton Keynes, England, 1988.
- Piper, J. D. A., Palaeomagnetism, in *Geomagnetism*, edited by J. A. Jacobs, pp. 31-161, Academic, San Diego, Calif., 1989.
- Quennell, A. M., Tectonics of the Dead Sea rift, paper presented at Congreso Geológico Internacional, 20th session, Asoc. de Serv. Geol. Afri., Mexico City 1956.
- Ramdohr, P., *The Ore Minerals and their Intergrowths*, 1174 pp., Pergamon, New York, 1969.
- Refai, E., N. A. Wassif, and A. Shoaib, Stability of remanence and paleomagnetic studies of some chromite ores from Barramiya and Allawi occurrences, Eastern Desert, Egypt, *Earth Planet. Sci. Lett.*, 94, 151-159, 1989.
- Ron, H., and G. Baer, Paleomagnetism of Lower Cretaceous rocks from southern Israel, *Isr. J. Earth Sci.*, 37, 73-81, 1988.
- Ron, H., and Y. Kolodny, Paleomagnetic studies in Israeli rocks (Lower Cambrian Timna Formation, southern Israel) final report, Minist. of Energy and Infrastructure, Jerusalem, 1985.
- Ron, H., R. Freund, Z. Garfunkel, and A. Nur, Block-rotation by strike-slip faulting: Structural and paleomagnetic evidence, *J. Geophys. Res.*, 89, 6256-6270, 1984.
- Sallomy, J. T. and M. Krs, A paleomagnetic study of some igneous rocks from Jordan, in *Evolution and Mineralization of the Arabian-Nubian shield*, proceedings of a symposium, Inst. Appl. Geol. King Abdulaziz Univ., Jeddah, Kingdom of Saudi Arabia, Vol. 3, pp. 155-164, Pergamon, Oxford, 1980.

- Saradeth, S., H. C. Soffel, P. Horn, D. Muller-Sohnius, and A. Schult, Upper Proterozoic and Phanerozoic pole positions and potassium-argon (K-Ar) ages from the East Sahara Craton, *Geophys. J.*, **97**, 209-221, 1989.
- Scotese, C. R., and S. F. Barrett, Gondwana's movement over the south pole during the Palaeozoic: Evidence from lithological indicators of climate, Palaeozoic Palaeogeography and Biogeography, *Geol. Soc. Mem.*, London, **12**, 75-85, 1990.
- Segev, A., Lithofacies relations and mineralization occurrences in the Timna formation, Timna Valley, (in Hebrew, English abstract), Ph.D. thesis, Hebrew University of Jerusalem, 1985.
- Segev, A., and E. Sass, Lithofacies and thickness control by epigenetic dissolution—The dolomitic Timna Formation, Cambrian, southern Israel, *Sedimenta.Geol.*, **63**, 109-126, 1989.
- Segev, A., M. Rybakov, T. Weissbrod, and M. Beyth, The Lower Cretaceous magmatic activity in the Timna Valley: Evidence from a detailed magnetic survey, paper presented at annual meeting, Isr. Geol. Soc. Ashqelon, **130**, 1992.
- Shpitzer, M., M. Beyth and A. Matthews, Igneous differentiation in the late Precambrian plutonic rocks of Mt. Timna, *Isr. J. Earth Sci.*, **40**, 17-27, 1991.
- Strangway, D. W., R. M. Honea, B. E. McMahon, and E. E. Larson, The magnetic properties of naturally occurring goethite, *Geophys. J. R. Astron. Soc.*, **15**, 345-359, 1968.
- Vail, J. R., Pan African crustal accretion in northeast Africa, *J. Afr. Earth Sci.*, **1**, 285-294, 1983.
- Van der Voo, R., Reliability of paleomagnetic data, *Tectonophysics*, **189**, 1-9, 1990.
- Zijderveld, J. D. A., A.C. demagnetization of rocks: Analysis of results, in *Methods in Paleomagnetism*, edited by D. W. Collinson, K. M. Creer, and S. K. Runcom, pp. 254-286, Elsevier, New York, 1967.
- Zlatkin, A., and U. Würzburger, Eruptive rocks of Timna (Negev), *Isr. Geol. Surv. Bull.*, **14**, 41, 1957.

M. Beyth, Geological Survey of Israel, 30 Malkhe Yisrael St., Jerusalem 95501, Israel.

S. Marco, A. Matthews, O. Navon, Institute of Earth Sciences, The Hebrew University, Jerusalem 91904, Israel.

H. Ron, Institute for Petroleum Research and Geophysics, P.O.B. 2286, Holon 58122, Israel.

(Received July 10, 1992;
revised May 7, 1993;
accepted May 24, 1993.)